analytical chemistry

Article

pubs.acs.org/ac

Sequential Identification of Model Parameters by Derivative Double Two-Dimensional Correlation Spectroscopy and Calibration-Free Approach for Chemical Reaction Systems

Nicolas Spegazzini,*[,†] Heinz W. Siesler,[‡] and Yukihiro Ozaki[†]

[†]Department of Chemistry, School of Science and Technology, Kwansei Gakuin University, Gakuen 2-1, Sanda, Hyogo 669-1337, Japan

[‡]Department of Physical Chemistry, University of Duisburg-Essen, D 45117 Essen, Germany

Supporting Information

ABSTRACT: A sequential identification approach by two-dimensional (2D) correlation analysis for the identification of a chemical reaction model, activation, and thermodynamic parameters is presented in this paper. The identification task is decomposed into a sequence of subproblems. The first step is the construction of a reaction model with the suggested information by model-free 2D correlation analysis using a novel technique called derivative double 2D correlation spectroscopy (DD2DCOS), which enables one to analyze intensities with nonlinear behavior and overlapped bands. The second step is a model-based 2D correlation analysis where the activation and thermodynamic parameters are estimated by an indirect implicit calibration or a calibration-free approach. In this way, a minimization process for the spectral information by sample−sample 2D correlation spectroscopy and kinetic hard modeling (using ordinary differential equations) of the chemical reaction model is carried out. The sequential identification by 2D correlation analysis is illustrated with reference to the isomeric structure of diphenylurethane synthesized from phenylisocyanate and phenol. The reaction was investigated by FT-IR spectroscopy. The activation and thermodynamic parameters of the isomeric structures of diphenylurethane linked through a hydrogen bonding equilibrium were studied by means of an integration of model-free and model-based 2D correlation analysis called a sequential identification approach. The study determined the enthalpy (ΔH = 15.25 kJ/mol) and entropy ($T\Delta S$ = 13.20 kJ/mol) of C═O···H hydrogen bonding of diphenylurethane through direct calculation from the differences in the kinetic parameters ($\delta\Delta^{\ddagger}H$, $-T\delta\Delta^{\ddagger}S$) at equilibrium in the chemical reaction system.

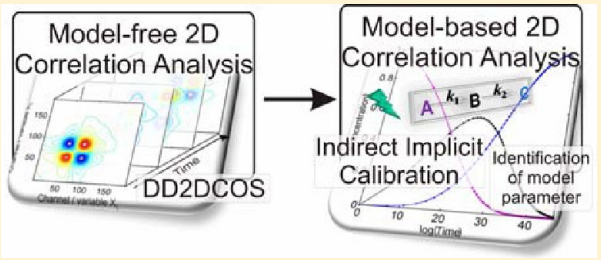

Significant advances in the study of chemical reaction systems are highly dependent on the meaningful extraction of chemical knowledge from large amounts of experimental data. Such experimental data for chemical reaction systems can be obtained by using a variety of techniques. Among them, the vibrational spectroscopies [Raman, mid-infrared (IR), and near-infrared (NIR)] are specific, potential tools for this purpose.[1] Raman, IR, and NIR spectroscopy have recently been extensively used due to their sensitivity to molecular structure and conformation and their usefulness in studying reaction mechanisms.[2−4] For obtaining real-time information about chemical composition, IR spectroscopy has proven to be highly versatile, especially when performed with the attenuated total reflection (ATR) technique. ATR probes allow the acquisition of precise information about chemical components with short optical path lengths (0.5−3 μm), and the fiber cables provide a higher flexibility for positioning the spectrometer relative to the sample compared to metallic lightguides.[5−7]

Dynamic models are used to analyze, monitor, control, and optimize a reaction system.[8] These models are often based on first principles and describe the evolution of the states (number of moles, temperature, and volume) by means of conservation equations of differential nature and constitutive equations of algebraic nature. However, systematic and general methodology for the effective analysis and interpretation of "complex-mixture" spectroscopic data to gain meaningful physical and chemical insight into reactive systems is still limited.[9] Although the identification methods of the above systems are useful for any arbitrary reaction system,[10] the issues above are particularly relevant to the most general and widespread problem in the chemical sciences, namely, system identification in chemical reaction modeling.[11−15]

Two-dimensional (2D) correlation spectroscopy (2DCOS) has gained great interest among scientists in a variety of research fields over the last two decades or so,[16−19] since it was first proposed by Noda in 1986.[20−23] The basic concept of 2D correlation spectroscopy is to depict a correlation contour map by introducing a simple correlation analysis to a stimulated spectral fluctuation (called dynamic spectra) caused by a certain

Received: July 5, 2012
Accepted: August 27, 2012
Published: August 27, 2012

   dx.doi.org/10.1021/ac301867u | *Anal. Chem.* 2012, 84, 8330−8339

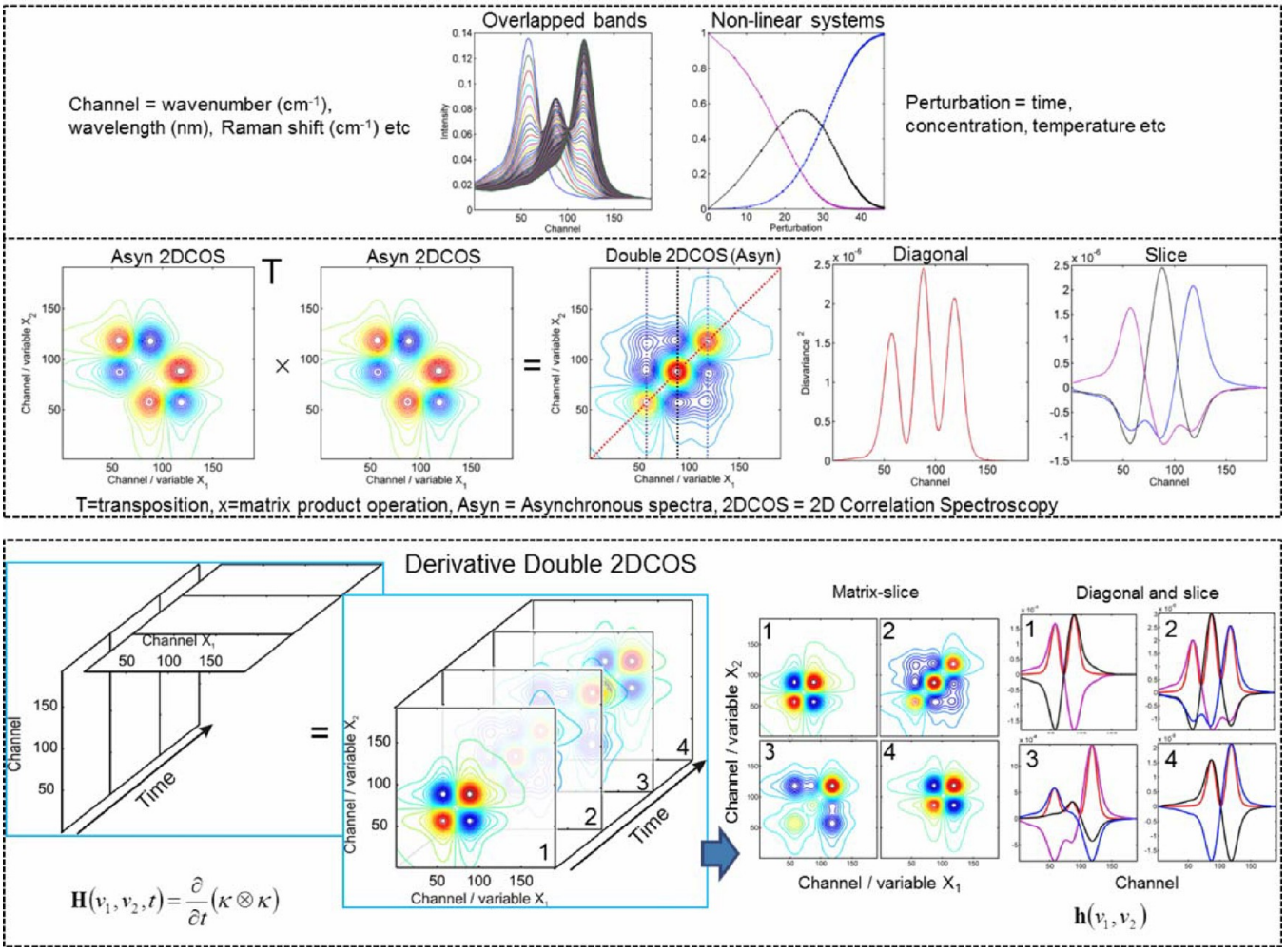

Figure 1. Simulated spectra comprising three overlapped bands with different rates and their corresponding nonlinear perturbations (top). Schematic representation of D2DCOS spectra generated from 2D asynchronous $\Psi^{T}\Psi$ (middle). Schematic representation of DD2DCOS spectra-generated correlation of the intensity slopes when the derivative was applied (bottom).

perturbation, which may be an electrical, thermal, magnetic, chemical, acoustic, or mechanical stimulation.[23] 2D correlation spectroscopy has provided a new area in the field of molecular structure studies by spreading an overlapped one-dimensional (1D) spectrum to the second dimension. Subtle changes in the 1D spectrum, often buried in complicated spectral features of a real chemical system, can be visualized in terms of cross-peaks in 2D correlation maps.[23]

In the last two decades there have been a number of new developments in 2DCOS. They can be classified into two major branches, model-free 2D correlation and model-based 2D correlation. Model-free 2D correlation analysis provides an unbiased model-free procedure that allows one to extract directly pertinent information from a spectral data set.[16−18,23] On the other hand, a model-based 2D correlation provides a broader scope than that from the current limitations of correlation analysis.[16−18,23] Unlike the strictly phenomenological data treatment of conventional 2D correlation analysis, model-based 2D correlation can bring forth the idea of hypothesis testing and even the determination of causal relationship within the data analysis, at least within the boundary of the proposed model structure.

One can find two kinds of ideas in model-based 2D correlation analysis. The first, proposed by Eads and Noda for nuclear magnetic resonance (NMR) spectra, introduced the concept that can be considered to be a form of hetero-correlation analysis, where one of the data sets is a collection of model calculations with systematically varying adjustable parameters. The highest correlation is achieved when the model parameter matches closest to the actual data; this method is referred to as the 2D waveform correlation analysis.[24] The second was developed by Dluhy and co-workers[25,26] who reported a series of works that enable the investigation of the correlations between spectral data and a set of kernel functions called the $\beta\nu$ and $k\nu$ correlation. Recently, Noda designed the concept of asynchronous kernel analysis (derived from the idea of kernel functions) as a model-free analysis based on bilinear decomposition,[27] where it is possible to obtain spectral and relative information about the species combined by self-modeling curve resolution or multivariate curve resolution methods.[28] However, all these methods do not allow for the identification and extraction of model parameters (concentration, kinetic constants, activation, and thermodynamic parameters).

We propose a 2D correlation methodology in order to extract information about chemical systems based on a band assignment of dynamic spectra to obtain model parameters. This is a reduction to an identification problem, and it is

dx.doi.org/10.1021/ac301867u | Anal. Chem. 2012, 84, 8330−8339

possible to decompose the problem into a sequence of subproblems (sequential identification) using the goodness of model-free and model-based 2D correlation analysis. This proposed methodology is used here to investigate the sequential identification of model parameters in order to extract the activation and thermodynamic parameters in a chemical reaction system. In what follows, several steps will be discussed: (1) A new technique named derivative double 2D correlation spectroscopy (DD2DCOS) is used for the construction of a chemical reaction model (the number of reactions and species) based on the information extracted from the model-free 2D correlation analysis. DD2DCOS has provided a new approach in the field of molecular structure studies by spreading an overlapped 2D spectrum to the third dimension using the slices (2D spectra) for easy visualization (Figure 1). The DD2DCO analysis opens up the possibility of studying systems with nonlinear behavior and provides information among the correlation spectroscopy variables; the signal over time has nonlinear behavior. In our case, it is in the direction of the reaction progress in the second-order reaction. Another advantage is that it used the benefits of double 2DCOS (D2DCOS) which was carried out by a series of simple matrix multiplication operations among asynchronous spectra and allowed for the study of the spectral intensities of overlapped bands which change in the same direction. Thus, it is possible to enhance the selectivity and the spectral resolution by the 2DCOS analysis (Figure 1). (2) In the approach for the determination of activation and thermodynamic parameters of the model, a reaction mechanism is postulated in the first step, giving a system of simultaneous ordinary differential equations (ODEs). Using known initial conditions, the ODEs are numerically integrated to estimate time-dependent concentration profiles. The concentration profiles (reaction extent profiles) are fitted directly to the covariance reaction spectra in the concentration space by sample−sample 2D correlation (SS-2DCO) analysis,[29] where each point in the SS-2DCO analysis represents the covariance between a given pair of sample traces such as those measured at different reaction times, thereby making explicit calibration unnecessary. This approach is called implicit calibration by Taavitsainen's convention.[30,31] Since the determination of the counterpart of the data in this approach does not require any additional external information, it is also deservedly referred to as a calibration-free approach in the literature.[15,32,33]

In the present study, we apply our proposed method to the reaction of phenol with phenylisocyanate to synthesize diphenylurethane. The reaction was monitored by NIR spectroscopy, demonstrating the applicability of remote analysis over a distance of 90 m between a NIR spectrometer and the measuring position.[34] Fiber-optic coupled FT-IR/ATR spectroscopy was also applied to study the same reaction.[35,36] It was shown in the FT-IR/ATR study that the evolution of a ν(C═O) band doublet, due to free and hydrogen-bonded carbonyl groups of the diphenylurethane product, was explained by the possible presence of two isomeric structures (Scheme 1) where one forms hydrogen bonds with itself or with the OH group of the reactant phenol.

In this work, the isomeric structures of diphenylurethane are analyzed by sequential identification of model parameters by 2D correlation analysis, during the synthesis of diphenylurethane from phenylisocyanate and phenol at different temperatures. Sequential estimation by 2D correlation analysis allows a global problem to be addressed through the decomposition of a problem into a sequence of subproblems (sequential identification). From this calibration-free methodology we derived activation and thermodynamic parameters directly from the 2D correlation spectroscopy analysis.

Scheme 1. Synthesis of Diphenylurethane from Phenylisocyanate and Phenol and the Isomeric Structure of Diphenylurethane

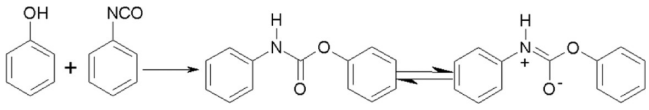

We studied the enthalpy and entropy of diphenylurethane C═O···H hydrogen bonding by direct calculation of the differences in the activation parameters ($\delta\Delta^{\ddagger}H$, $-T\delta\Delta^{\ddagger}S$) at equilibrium in the chemical reaction system, where the model parameters have never before been obtained through 2DCOS analysis. This methodology could lead to a better understanding of the different functions and interactions of hydrogen bonding in supramolecular systems.

THEORY

Sequential Identification of Model Parameters by 2D Correlation Analysis. The approach of the sequential identification by 2D correlation analysis is applied to determine the parameters of the chemical reaction system. The procedure is summarized by the following derivations and equations.

FT-IR Spectroscopic Data. Let $\mathbf{Y}$ ($me \times n$) represent the consolidated spectroscopic data matrix where m denotes the number of spectra taken in one step of a batch experiment (each step has an initial condition), e indicates the number of batch steps, and n represents the number of data channels associated with the spectroscopic range. On the basis of Beer−Lambert's law, $\mathbf{Y}$ can be assumed to result from a linear combination (eq 1) of concentration matrix $\mathbf{C}$ ($me \times s$) and the pure-component spectra matrix $\mathbf{A}$ ($s \times n$) (where s denotes the number of observable species in the chemical mixture), and $\mathbf{E}$ ($me \times n$) is the experimental and instrumental error (eq 1).

$$\mathbf{Y} = \mathbf{C}\cdot\mathbf{A} + \mathbf{E} \tag{1}$$

Changes of Moles. The equation of Jouguet-de Donder for the description of the evolution of chemical species, $\Delta\mathbf{C} = \mathbf{X}\cdot\mathbf{N}\cdot\mathbf{V}_L^{-1}$, can be seen as the change of moles of observable species $\Delta\mathbf{C}$, defined in terms of reaction extents, $\mathbf{X}$, the reaction stoichiometries, $\mathbf{N}$, and the volume, $\mathbf{V}_L^{-1}$, in liters. Combined with the Beer−Lambert law (eq 1), the two equations can be modeled as a linear combination, as shown in eq 2:

$$\Delta\mathbf{Y} = \mathbf{Y} - \mathbf{1}_p\mathbf{y}_0 = \mathbf{C}\cdot\mathbf{A} - \mathbf{1}_p\mathbf{c}_0\cdot\mathbf{a}_0 = \Delta\mathbf{C}\cdot\mathbf{A} = \mathbf{X}\cdot\mathbf{N}\cdot\mathbf{A}$$

$$\Delta\mathbf{Y} = \mathbf{X}\cdot\mathbf{N}\cdot\mathbf{A} = \mathbf{X}\cdot\mathbf{\Gamma} \tag{2}$$

where $\mathbf{1}_p$ is the p-dimensional vector filled with ones and $\mathbf{y}_0$ represents the initial conditions in the first spectrum of the starting materials. The reaction spectral matrix is denoted by $\mathbf{\Gamma}$.

Model-Free 2D Correlation Analysis. The classic synchronous and asynchronous spectra[23] are constructed according to eq 2, where spectral (sd) and reaction extent dimension (ed) can be expressed in the matrix notation as

$$\mathbf{\Phi}_{sd} = \left(\frac{1}{m-1}\right)\Delta\tilde{\mathbf{Y}}^{T}\cdot\Delta\tilde{\mathbf{Y}} \quad \text{or} \quad \mathbf{\Phi}_{ed} = \left(\frac{1}{n-1}\right)\Delta\tilde{\mathbf{Y}}\cdot\Delta\tilde{\mathbf{Y}}^{T} \tag{3}$$

dx.doi.org/10.1021/ac301867u | Anal. Chem. 2012, 84, 8330−8339

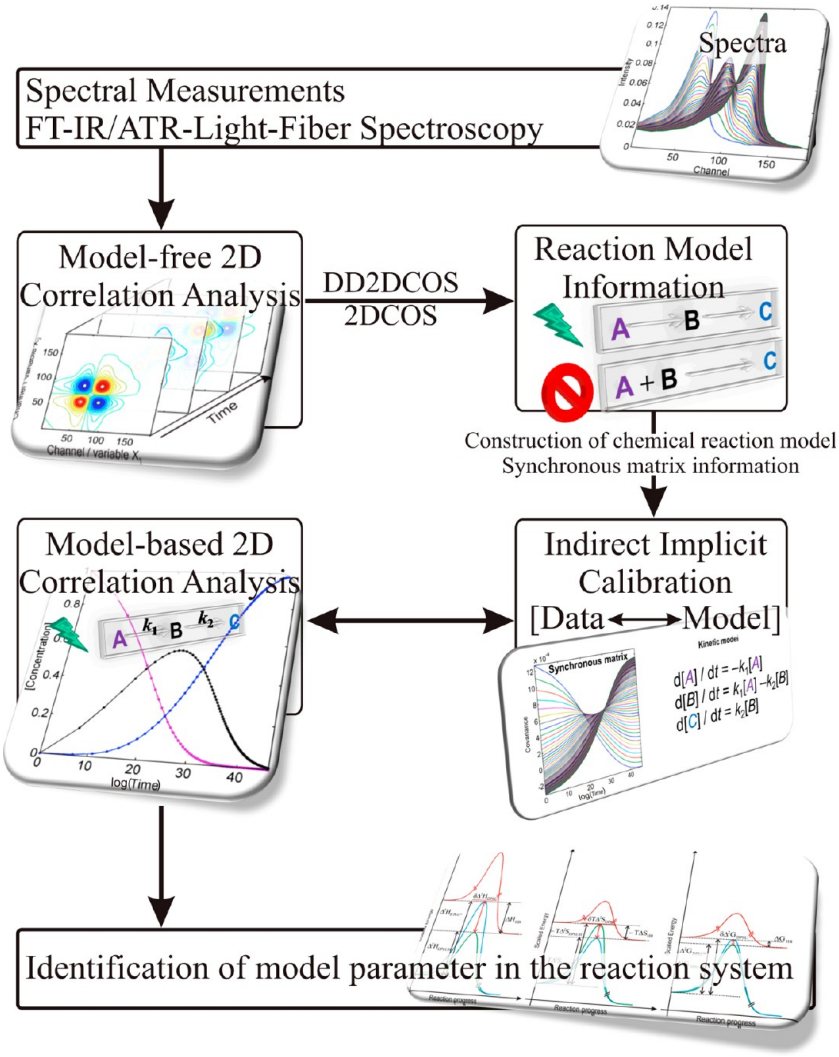

Figure 2. Schematic of the sequential identification approach by 2D correlation analysis.

$$\mathbf{\Psi}_{sd} = \left(\frac{1}{m-1}\right)\Delta\tilde{\mathbf{Y}}^{T}\cdot\mathbf{N}\cdot\Delta\tilde{\mathbf{Y}} \quad \text{or}$$
$$\mathbf{\Psi}_{ed} = \left(\frac{1}{n-1}\right)\Delta\tilde{\mathbf{Y}}\cdot\mathbf{N}\cdot\Delta\tilde{\mathbf{Y}}^{T} \tag{4}$$

where $\Delta\tilde{\mathbf{Y}}$ denotes the dynamic spectra equivalent to the mean-centering matrix $\Delta\mathbf{Y}$ and $\mathbf{N}$ is the Hilbert–Noda transformation matrix (and also T denotes the transpose of the matrix). In general, the element in the $\mathbf{\Phi}$ synchronous correlation intensity represents the in-phase or coincidental variations of the infrared difference spectra, while that in the $\mathbf{\Psi}$ asynchronous correlation intensity represents the out-of-phase nature of the IR difference spectra during the observation period of the reaction. After a brief introduction to the classic 2D correlation analysis, we introduce in the first step (Figure 2) a new powerful tool named DD2DCOS based on D2DCOS (see Figure S-1 of the Supporting Information).[37] The idea for D2DCOS is to enhance the selectivity and the spectral resolution. It is capable of distinguishing overlapped bands, even when their intensities change in the same direction and can be expressed in matrix notation as (Figure 1)

$$\mathbf{K} = \mathbf{\Psi}_{sd}^{T}\cdot\mathbf{\Psi}_{sd} \tag{5}$$

However, it is only applicable when the increment of the intensities is linear. Thus, DD2DCOS allows the study of systems with nonlinear behavior and provides information among correlation spectroscopy variables; the signal over time has a nonlinear behavior. This analysis is based on the correlation of the intensity slopes (see Figure S-2 of the Supporting Information) when a derivative is applied through forward finite difference methods or polynomial methods like Savitzky–Golay.[38]

$$\mathbf{H} = \frac{\partial}{\partial t}(\kappa \otimes \kappa) \tag{6}$$

where $\mathbf{H}$ is a hypermatrix that allows for the extraction of a slice (matrix) to analyze the correlation slopes of the difference intensities as a function of time (Figure 1), and $\otimes$ denotes the Kronecker product. In our case, it is in the direction of the reaction progress of the second-order reaction. Another advantage is that it uses the benefits of D2DCOS and allows for the study of spectral intensities of overlapped bands which change in the same direction. Thus, it is possible to enhance the selectivity and the spectral resolution by 2DCOS analysis.

Using the spectral information extracted by the model-free 2D correlation analysis, one can construct a chemical reaction model for the next step in the identification of model

dx.doi.org/10.1021/ac301867u | Anal. Chem. 2012, 84, 8330–8339

parameters (model-based 2D correlation analysis) by implicit calibration.

Model-Based 2D Correlation Analysis. In this step, model parameter identification is performed with the spectral information of the reaction extracted in the model-free 2D correlation analysis: (1) synchronous matrix, $\mathbf{\Phi}_{ed}$, in the reaction extent space and (2) construction of chemical reaction model based on the reaction extents by the ODE and stoichiometric model **N**. The implicit calibration is considered to be a minimization problem between the data and simulations.

Implicit Calibration. The idea of implicit calibration or the calibration-free approach is a minimization of spectral information and kinetic hard modeling of the chemical reaction model. The calibration step is performed separately inside the kinetic parameter estimation loop. The calibration of measured spectra is done using the concentrations calculated with an iteratively improved kinetic parameter. The gradient-based Newton−Gauss−Levenberg/Marquardt algorithm (NGL/M) is used to solve this nonlinear regression. A description of this method is provided in the Supporting Information.

There are basically two approaches for the implicit calibration. Direct implicit calibration spectra are considered as measured variables, and the fit is done in absorbance units. If the spectra are denoted **Y** and the concentrations calculated by the kinetic model (ODE) are denoted $\mathbf{C}_\theta$, the calibration model is $\mathbf{Y} = \mathbf{C}_\theta\mathbf{B}$, where **B** is a matrix regression. It is possible to obtain **B** by partial least-squares (PLS) or principal component regression (PCR); the procedure can be briefly described by the pseudoinverse of $\mathbf{C}_\theta$, $\mathbf{B} = \mathbf{C}_\theta^{+}\mathbf{Y}$, by replacing $\mathbf{Y}_\theta = \mathbf{C}_\theta\mathbf{C}_\theta^{+}\mathbf{Y}$. Now, the estimates for the kinetic parameter, θ, are obtained iteratively by minimizing the least-squares norm, $\|\mathbf{Y} - \mathbf{Y}_\theta\| = \|\mathbf{Y} - \mathbf{C}_\theta\mathbf{C}_\theta^{+}\mathbf{Y}\|$.

In indirect implicit calibration, the calculated concentrations are considered to be the "measured" variables, and the fitting is performed in concentration units. This is actually a multivariate calibration with "floating" data.[31] Thus, in this approach, the calibration model is $\mathbf{C}_\theta = \mathbf{YB}$, where **B** is a regression matrix that one can obtain by PLS or PCR, and the procedure can be briefly described by the pseudo inverse of **Y**, $\mathbf{B} = \mathbf{Y}^{+}\mathbf{C}_\theta$, by replacing $\mathbf{C}_{cal} = \mathbf{YY}^{+}\mathbf{C}_\theta$. Now the estimates for the kinetic parameter, θ, are obtained iteratively by minimizing the least-squares norm, $\|\mathbf{C}_\theta - \mathbf{C}_{cal}\| = \|\mathbf{C}_\theta - \mathbf{YY}^{+}\mathbf{C}_\theta\|$. It is remarkable in the following that, altogether, two different concentration profiles are used: $\mathbf{C}_\theta$, the modeled concentration profiles by the ODE obtained using the current value of the kinetic parameters, θ, and $\mathbf{C}_{cal}$, the calibrated concentration profiles obtained from the calibration step in the indirect implicit calibration, where both concentrations are dependent on the current value of the kinetic parameter, θ.

When $\mathbf{C}_\theta$ is modeled, using the Target Testing method proposed by Furusjö et al.[39] projects $\mathbf{C}_\theta$ onto the **U** left eigenspace from singular-value decomposition of **Y**. But in our case, when $\mathbf{X}_\theta$ is modeled using the ODE by the indirect implicit calibration, the projections, $\mathbf{X}_\theta$ onto the synchronous matrix $\mathbf{\Phi}_{ed}$ in the reaction extent space, reduce the effects of baseline shifts and improve the contribution of each component to the data during the fitting; it can be regarded as an indirect kinetic hard-modeling by implicit calibration using PCR. This is shown by reducing the matrix $\mathbf{\Phi}_{ed}$ to

$$\mathbf{\Phi}_{ed} = \bar{\mathbf{U}}\cdot\bar{\mathbf{S}}^2\cdot\bar{\mathbf{U}}^{T} \tag{7}$$

by singular-value decomposition (SVD) ($\bar{\mathbf{U}}$ and $\bar{\mathbf{S}}$ are the reduced matrices form) in the objective function described before and replacing it by its expression derived in

$$\|\mathbf{X}_\theta - \mathbf{\Phi}_{ed}\mathbf{X}_\theta\| = \|(\mathbf{I} - \mathbf{\Phi}_{ed})\mathbf{X}_\theta\| \tag{8}$$

The parameter identification for the chemical reaction system is obtained by a nonlinear least-squares minimization problem between the synchronous matrix, $\mathbf{\Phi}_{ed}$, in the reaction extent space and the simulation, $\mathbf{X}_\theta$ (by the ODE), to fit the kinetic parameter and **I** is called identity matrix (eq 8).

Finally, the concentration and the pure spectra for each species can be calculated by eq 9.

$$\mathbf{C} = (\mathbf{1}_p\mathbf{c}_0 + \Delta\mathbf{C})\cdot\mathbf{V}_L^{-1}$$

$$\mathbf{A} = \mathbf{C}^{+}\cdot\mathbf{Y} \tag{9}$$

where $\mathbf{1}_p$ is the p-dimensional vector filled with ones and $\mathbf{c}_0$ represents the initial concentration of the starting materials. The pseudoinverse of **C** is denoted by $\mathbf{C}^{+}$.

Arrhenius−Eyring Approach. To carry the analysis further, the Arrhenius data from the perspective of transition state theory are considered to obtain values for the enthalpy and entropy of activation, $\Delta^{\ddagger}H$ and $\Delta^{\ddagger}S$, respectively. In this context, we use the approximations in solution shown in eq 10:

$$k = A\, e^{-E_a/RT}$$

$$E_a \approx \Delta^{\ddagger}H + RT$$

$$A \approx e^{1}\frac{k_B T}{h}\, e^{\Delta^{\ddagger}S/R} \tag{10}$$

where R is the gas constant, k_B is the Boltzmann constant, and h is Planck's constant.[40]

Next, from Eyring to the van't Hoff equation, relating the kinetic parameters to the thermodynamic parameters and applying the Eyring equation, k can be written as

$$k = \frac{k_B T}{h}\, e^{-\Delta^{\ddagger}H/RT}\, e^{\Delta^{\ddagger}S/R} \tag{11}$$

and in further iterations the thermodynamic parameters can be determined, and finally the equation of van't Hoff can be deduced:

$$\ln\frac{k_r}{T} - \ln\frac{k_f}{T} = -(\Delta^{\ddagger}H_{DPhU} - \Delta^{\ddagger}H_{DPhUH})\frac{1}{RT} + \left(\ln\frac{k_B}{h} - \ln\frac{k_B}{h}\right) + (\Delta^{\ddagger}S_{DPhU} - \Delta^{\ddagger}S_{DPhUH})\frac{1}{R}$$

$$\ln\frac{k_r}{k_f} = -\left(\frac{\delta\Delta^{\ddagger}H}{R}\right)\left(\frac{1}{T}\right) + \frac{\delta\Delta^{\ddagger}S}{R} \approx \ln K_d = -\left(\frac{\Delta H_{HB}}{R}\right)\left(\frac{1}{T}\right) + \frac{\Delta S_{HB}}{R} \tag{12}$$

This approach is allowed because the system must be in equilibrium. Starting from this basis, we can deduce, by the difference on both sides, an approximate delta activation parameter that is equivalent to a thermodynamic parameter.

EXPERIMENTAL SECTION

Here, the FT-IR/ATR experiments of the diphenylurethane reaction for empirical data collection are briefly summarized. For further detail, the readers are referred to the descriptions in our previous papers.[35,36] Each reaction was performed in a 250 mL four-neck round-bottom flask with an attached reflux condenser and a magnetic stirrer. Two quick-fits were used to hold an ATR probe, and a contact thermometer was used to

dx.doi.org/10.1021/ac301867u | Anal. Chem. 2012, 84, 8330−8339

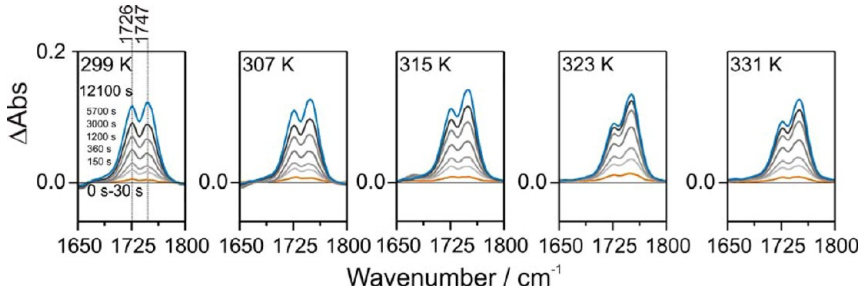

Figure 3. Experimental time-resolved FT-IR spectra in the region of 1650−1800 cm^{-1} for the prominent doublet of hydrogen-bonded and free-form ν(C═O) absorption bands observed at 1726 and 1747 cm^{-1}, respectively.[34].

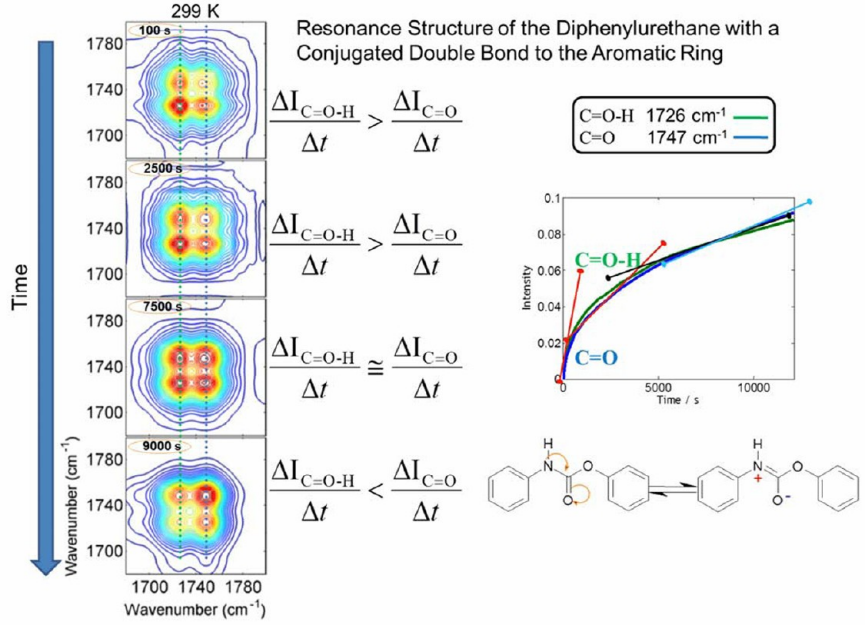

Figure 4. DD2DCOS spectra for the reaction at 299 K for 100, 2500, 7500, and 9000 s.

control the reaction temperature. A fourth opening in the flask was used to add reagents. In the flask, 9.88 g of phenol was dissolved in chloroform (1.05 mol/L), 0.3 g of anhydrous $AlCl_3$ catalyst[35,36] was added, and the solution was heated to one of the desired reaction temperatures (299, 307, 315, 323, or 331 K). When the temperature was reached, a spectrum was recorded, and subsequently 11.91 g (1.00 mol/L) of phenylisocyanate was added to the mixture.

Spectroscopic measurements were taken with a Bruker IFS-28 FT-IR spectrometer (Bruker Optik GmbH, Ettlingen, Germany) equipped with an MCT detector and a diamond ATR-probe (two reflections), which was coupled to the spectrometer by a 2 m silver halide waveguide fiber (Infrared Fiber Sensors, Aachen, Germany). IR spectra in the range of 850−1800 cm^{-1} were recorded at preselected time intervals (29 spectra in total) with a spectral resolution of 4 cm^{-1}, and 32 scans were co-added to achieve a good signal-to-noise ratio.

Computational Methods. SVD was performed using a linear algebra package library (LAPACK), and all calculations of ordinary differential equations were solved using ODE45, by Runge−Kutta methods integrated numerically using MATLAB functions. The gradient-based Newton−Gauss−Levenberg/Marquardt algorithm was used to solve the nonlinear regression for the identification of model parameters (see the Supporting Information). All calculations from the 2D correlation analysis were implemented by means of in-house routines of MATLAB, version 7.12 for Mac OS X (The MathWorks, Natick, MA).

RESULTS AND DISCUSSION

FT-IR/ATR Spectra. Figure 3 shows the FT-IR/ATR spectra of the reaction of phenylisocyanate and phenol to yield diphenylurethane in a chloroform solution at different temperatures (299, 307, 315, 323, or 331 K). A prominent doublet representing the hydrogen-bonded and the free ν(C═O) absorption bands at 1726 and 1747 cm^{-1}, respectively, was observed in each case. The non-hydrogen-bonded ν(C═O) absorption band at 1747 cm^{-1} shows a stronger relative intensity with increasing temperature.

Model-Free 2D Correlation Analysis. *Determination of a Reaction Model.* DD2DCOS allows studies of systems with nonlinear behavior and provides information between correlation spectroscopy variables; a signal over time has a nonlinear behavior. This is calculated by eq 6 of the hypermatrix, **H**, which allows the extraction of a slice (matrix) for analyzing the correlation slopes of the difference intensities as a function of time. In our case, the hydrogen-bonded and free ν(C═O) absorption bands at 1726 and 1747 cm^{-1}, respectively, are developed in the direction of the reaction progress of the second-order reaction.

dx.doi.org/10.1021/ac301867u | *Anal. Chem.* 2012, 84, 8330−8339

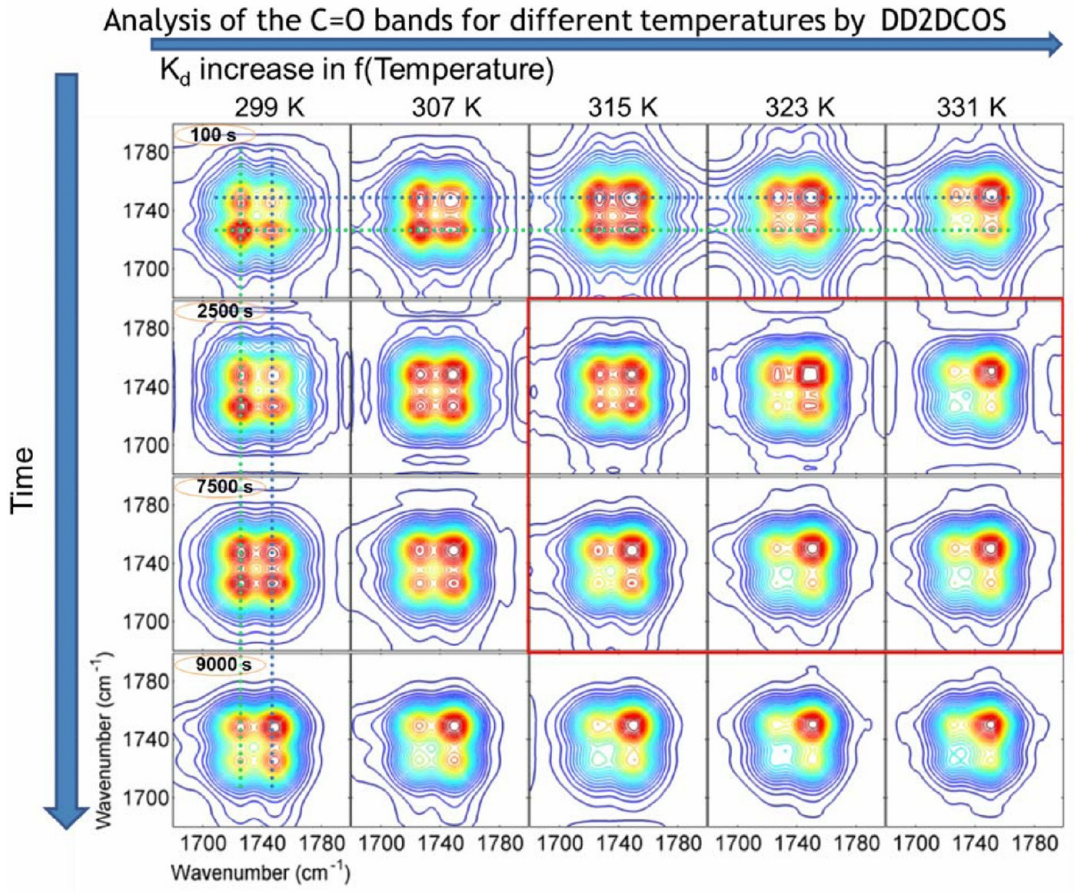

Figure 5. DD2DCOS spectra for the reaction at 299, 307, 315, 323, and 331 K for 100, 2500, 7500, and 9000 s.

Figure 4 depicts four slices (matrix) for the reaction at 299 K for 100, 2500, 7500, and 9000 s (from top to bottom) in which the correlation of the slopes of intensities can be found as a function of time; in the first 100 s the absorption band at 1726 cm^{-1} is slightly larger compared to that at 1747 cm^{-1}. At 2500 s, this phenomenon slightly decreases for the correlation of the intensity slopes at 1726 cm^{-1} but is also equivalent to that of the first 100 s. However, at 7500 s the correlation of the slopes of intensities is almost equivalent, and finally, at 9000 s the correlation is reversed and the band at 1747 cm^{-1} is larger. For more information, we calculated DD2DCOS in the whole range, and we selected this region for the study. For any ambiguity in the 2D maps, please see Figures S-3 and S-4 of the Supporting Information.

Figure 5 displays four slices (matrix) for the reaction at different temperatures. For the early stage, the behavior is almost the same but the correlation of the slopes of intensities at 1747 cm^{-1} is larger compared to that at 1727 cm^{-1}. For the reaction at 307 K, the changes are similar to those at 299 K. The major changes for this reaction from 315 to 331 K lie between 2500 and 7500 s (red square). The correlation of the slopes of intensities at 1747 cm^{-1} increases significantly with increasing temperature. For any ambiguity in the 2D maps, we also tested DD2DCOS where noise is included for the sample at 299 K, and we obtained good results (see Figures S-5 and S-6 of the Supporting Information).

This temperature-dependent behavior suggests that the product, diphenylurethane, is in equilibrium between the free form (DPhU) and the hydrogen-bonded form (DPhUH) (Scheme 2).

Scheme 2. Isomeric Structures of Diphenylurethane from Phenylisocyanate and Phenol Linked in the Equilibrium with C═O···H−N Hydrogen Bonding

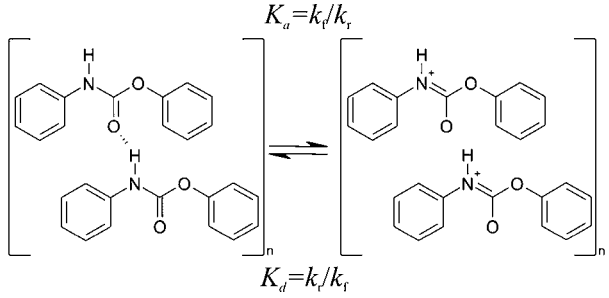

Model-Based 2D Correlation Analysis: Identification of Model Parameters by Implicit Calibration. Figure 6 shows the concentration profiles and mass balance of the reagents (PhOH, PhNCO) and the diphenylurethane product (DPhUH and DPhU) at different temperatures.

In a previous work by Friebe and Siesler, it was possible to observe an enhanced formation of DPhU compared to that of DPhUH as a function of temperature along the reaction progress.[35] The present results contrast with these findings by Friebe and Siesler, where a deviation was observed in the quantification between FT-IR/ATR and HPLC. The IR data showed higher concentration values than the liquid-chromatographic analysis for the reaction monitored at 331 K. This can be explained through a simultaneous overlap between the reaction and the equilibrium. For this reason, the reaction at

dx.doi.org/10.1021/ac301867u | Anal. Chem. 2012, 84, 8330−8339

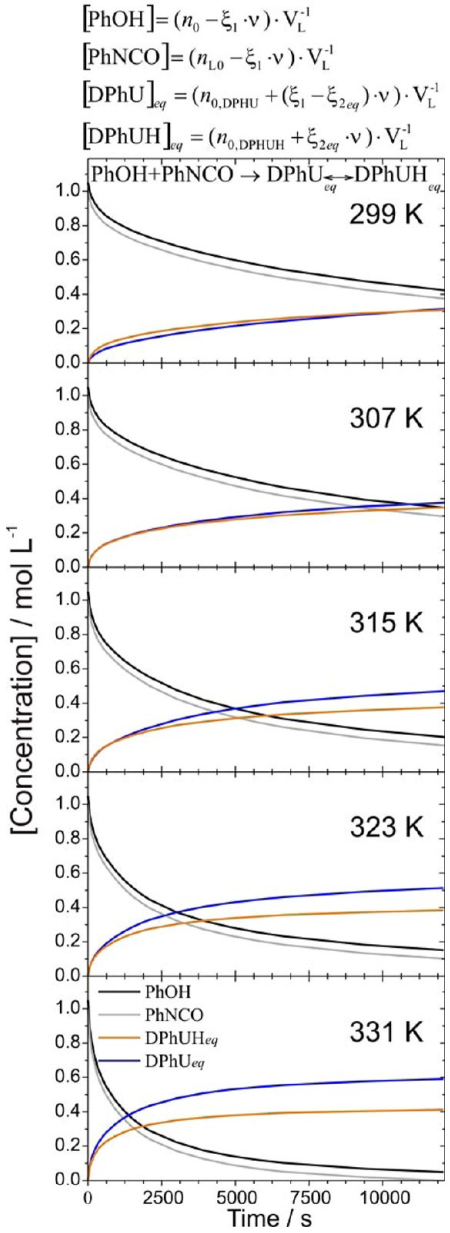

Figure 6. Concentration profiles for all species at different temperatures, in the synthesis of diphenylurethane with and without the hydrogen bond in the equilibrium.

331 K in ref 35 was considered an outlier in the Arrhenius treatment.

By contrast, it can be expected that with increasing temperature, the concentration of DPhU increases, whereas that of DPhUH decreases, controlled by a mass balance at different temperatures. This suggests that a kinetic model for these reactions would be controlled by the global equilibrium constant.

The relative proportions of the isomeric structures are controlled by the equilibrium and are given by the ratio of the two rates and, therefore, of the two rate constants in eq 13.

$$K_a = \frac{k_f}{k_r} = \frac{(n_{0,\mathrm{DPHUH}} + \xi_{2\mathrm{eq}}\nu)V_L^{-1}}{[n_{0,\mathrm{DPHU}} + (\xi_1 - \xi_{2\mathrm{eq}})\nu]V_L^{-1}} \text{ or } K_d = \frac{1}{K_a} \tag{13}$$

The ratio represents the kinetic control that drives the product distribution, and it is a common feature of these reactions. Moreover, the equilibrium constant between the formation of DPhU and DPhUH represents the instantaneous interchange of the hydrogen bond. Thus, these equilibria are a quantification of the association and dissociation of the hydrogen bond between the two isomers. In this case, the products reach equilibrium instantaneously, and since the proportion of products is determined by thermodynamics, their ratio is controlled by the standard Gibbs energies.

Assuming the dependence of the global equilibrium constant on the product, the data fitting (using eq 8) can be analyzed as one reaction with an equilibrium between the isomeric structures. This model corresponds to Scheme 3, as suggested

Scheme 3. Kinetic Model Linked with the Equilibrium of the Isomeric Structures of Diphenylurethane from the Reaction of Phenol and Phenylisocyanate

$$\mathrm{PhOH + PhNCO} \xrightarrow{k_1} \mathrm{DPhU} \underset{K_d = k_r/k_f}{\overset{K_a = k_f/k_r}{\rightleftharpoons}} \mathrm{DPhUH}$$

by the reaction extent modeling. On the other hand, we tested synchronous matrix information where noise is included for the sample at 299 K, and we show that the data fitting is robust to the noise. Also, the pure resolved spectra are obtained (see Figures S-7 and S-8 of the Supporting Information).

The ODEs based on the reaction extent of the model are shown as follows:

$$\begin{aligned} d\xi_1/dt &= k_1(n_{0,\mathrm{PhOH}} - \xi_1\nu)(n_{\mathrm{L0,PhNCO}} - \xi_1\nu) \\ &= k_1(n_{0,\mathrm{DPhU_{total}}} + \xi_1\nu) \\ d\xi_{2\mathrm{eq}}/dt &= k_f[n_{0,\mathrm{DPHU}} + (\xi_1 - \xi_{2\mathrm{eq}})\nu] \\ &= k_r(n_{0,\mathrm{DPHUH}} + \xi_{2\mathrm{eq}}\nu) \end{aligned} \tag{14}$$

Equation 14 describes an infinitesimal change (reaction rate) in the extent of the reaction (ξ) for the observable species, in a time interval, $t_0 \rightarrow t_n$. The change in the extent of the reaction expressed for reagents is the difference between the initial number of moles (n_0), moles of limiting reactant (n_{L0}), and the extent of the reaction. For the products, the change in the extent of the reaction is formally expressed as an addition between the initial number of moles and the extent of the reaction. The progress for the reaction, ξ_1, is associated with the formation of diphenylurethane for different temperatures, corresponding to the total moles of product. The other extent of the reaction, ξ_{2eq}, is associated with the equilibrium of the diphenylurethane, corresponding to the number of moles of diphenylurethane with hydrogen bonds. The difference in the extents of the reaction ($\xi_1 - \xi_{2eq} = \Delta\xi_{1,\,2eq}$) is proportional to the number of moles of diphenylurethane in the free form.

One can characterize the real concentrations of the global system of PhOH, PhNCO, DPhU, and DPhUH by the kinetic and equilibrium constants k_1, $K_a = k_f/k_r$, and $K_d = 1/K_a$. In this way, one can see that k_1 describes the formation of the amount of diphenylurethane, while K_a describes the relative proportion of the isomeric structures (Table 1).

The analysis of the equilibrium yields the kinetic constant ratio of k_f and k_r for the isomeric structures of diphenylurethane. This allows the computation of the association and dissociation constants for the hydrogen bonding of the

dx.doi.org/10.1021/ac301867u | Anal. Chem. 2012, 84, 8330−8339

Table 1. Calculated Rate and Association and Dissociation Kinetic Constants for the Synthesis of Hydrogen-Bonded (HB) and Non-Associated Diphenylurethane at Different Temperatures

	299 K	307 K	315 K	323 K	331 K
DPhU k_1 ($\times 10^{-4}$ M^{-1} s^{-1})	2.31 ± 0.14	3.25 ± 0.21	3.9 ± 0.72	5.03 ± 0.29	7.53 ± 0.30
$(k_f/k_r) = K_{a\_HB}$	(1.31/1.00) ± 0.12	(1.60/1.65) ± 0.01	(1.90/1.99) ± 0.05	(2.28/2.71) ± 0.02	(3.03/4.50) ± 0.01
$(k_r/k_f) = K_{d\_HB}$	0.76 ± 0.07	1.03 ± 0.16	1.06 ± 0.02	1.19 ± 0.10	1.49 ± 0.13

Table 2. Activation and Thermodynamic Parameters Obtained from the Arrhenius–Eyring and van't Hoff Plots for the Isomeric Structures of Diphenylurethane in Hydrogen-Bonding Equilibrium[a]

	E_a (kJ/mol)	$\Delta^{\ddagger}H$ (kJ/mol)	$\Delta^{\ddagger}S$ (J mol^{-1} K^{-1})	$T\Delta^{\ddagger}S$ (kJ/mol)	ΔH (kJ/mol)	ΔS (J mol^{-1} K^{-1})	$T\Delta S$ (kJ/mol)
DPhU	20.80 ± 4.00	33.39 ± 3.80	−209.7 ± 15.0	−62.70			
DPhUH	36.08 ± 3.50	18.19 ± 3.46	−258.6 ± 11.0	−77.30			
HB (K_d)					15.25 ± 2.41	44.15 ± 7.64	13.20

[a]The parameters are reported with a 95% confidence of bounds.

urethane structures. An increment of K_d is observed with temperature, as expected from the strong dependence of hydrogen bonding on temperature. This effect is proportional to the formation of DPhU. Our approach attempts to avoid potential artifacts arising from the practice of blindly equalizing. Due to the experimental error, a fit of the Arrhenius–Eyring and van't Hoff treatments has an r value close to 0.98 (see Figure S-9 of the Supporting Information).

The proposed model shows that at the time of the urethane synthesis, there is an overlap of the reaction extent between the formation of the isomeric structure (DPhU and DPhUH) and the balance of hydrogen bonding. This is observed through the activation parameters for each isomer of urethane. The difference between the activation parameters ($\Delta^{\ddagger}H_{DPhU} - \Delta^{\ddagger}H_{DPhUH}$ and $\Delta^{\ddagger}S_{DPhU} - \Delta^{\ddagger}S_{DPhUH}$) is proportional to the thermodynamic parameters ($\delta\Delta^{\ddagger}H_{DPhU} = \Delta H_{HB}$ and $\delta\Delta^{\ddagger}S_{DPhU} = \Delta S_{HB}$). The activation and thermodynamic parameters are summarized in Table 2. It should also be noted that the estimated value of the activation energy for DPhU is E_{a_DPhU} = 20.80 kJ/mol and E_{a_DPhUH} = 36.08 kJ/mol without excluding the reaction monitored at 331 K, and the value reported in a previous work reported by Friebe and Siesler is around E_a = 36 kJ/mol, calculated in a range from 299 to 323 K. This is due to a simultaneous overlap between the reaction and the equilibrium; the reaction at 331 K in ref 35 was considered an outlier in the Arrhenius treatment as mentioned above.

CONCLUSIONS

A sequential identification approach by a 2D correlation analysis has been presented for the model parameter identification of the chemical reaction systems. The identification problem is broken down into a sequence of simple subproblems, allowing stepwise identification of the model. In this work, we have proposed a methodology to extract information for the construction of the chemical reaction model using the notation reaction extent, in order to estimate model parameters. The approach proceeds in two steps. Step (1) involves the determination of the reaction model by model-free 2D correlation analysis. In this case, we use a novel idea called DD2DCOS, in which it is possible to have the correlation intensities for nonlinear behavior in our example second-order reaction, and moreover, it is also possible to enhance a spectral resolution for overlap bands, where the rate increases or decreases in the same direction. In step (2), the identification of the model parameter is performed by model-based 2D correlation analysis through indirect implicit calibration or a calibration-free approach, as a minimization problem between the chemical reaction model constructed by the ODE and the synchronous reaction extent information. The advantage of the indirect implicit calibration is that methods such as PLS and PCR can internally correct several kinds of spectral error, as long as the calibration data are representative with respect to these errors.[30,31]

Basically, this was the first time that quantitative information was extracted (activation and thermodynamic parameters) from the reaction system through a combination of experimental observations by FT-IR and modeling, based on sequential estimation as integration between model-free and model-based 2D correlation analysis. This calibration-free methodology could facilitate a better understanding of various functions and interactions in supramolecular systems like the "switching" of hydrogen bonds.

ASSOCIATED CONTENT

Supporting Information

Additional information as noted in the text. This material is available free of charge via the Internet at http://pubs.acs.org.

AUTHOR INFORMATION

Corresponding Author

*E-mail: nicolas.spegazzini@gmail.com.

Notes

The authors declare no competing financial interest.

ACKNOWLEDGMENTS

N.S. acknowledges support from the Japan Society for the Promotion of Science (JSPS) via a postdoctoral fellowship (Grant PE10056).

REFERENCES

(1) (a) Günzler, H.; Gremlich, H.-U. *IR Spectroscopy, An Introduction*; Wiley-VCH: Weinheim, Germany, 2002. (b) Siesler, H. W.; Ozaki, Y.; Kawata, S.; Heise, H. M. *Near-Infrared Spectroscopy Principles, Instruments, Applications*; Wiley-VCH: Weinheim, Germany, 2002. (c) Ferraro, J. R.; Nakamoto, K.; Brown, C. W. *Introductory Raman Spectroscopy*, 2nd ed.; Elsevier Science: Amsterdam, 2003.

(2) (a) Brewster, V. L.; Ashton, L.; Goodacre, R. *Anal. Chem.* **2011**, *83*, 6074–6081. (b) Ashton, L.; Johannessen, C.; Goodacre, R. *Anal. Chem.* **2011**, *83*, 7978–7983.

(3) Quaroni, L.; Zlateva, T.; Normand, E. *Anal. Chem.* **2011**, *83*, 7371–7380.

(4) Šašić, S.; Katsumoto, Y.; Sato, H.; Ozaki, Y. *Anal. Chem.* **2003**, *75*, 4010–4018.

(5) Heise, H. M.; Kuepper, L.; Butvina, L. N. *Anal. Bioanal. Chem.* **2003**, *375*, 1116−1123.
(6) Minnich, C. B.; Buskens, P.; Steffens, H. C.; Bäuerlein, P. S.; Butvina, L. N.; Küpper, L.; Leitner, W.; Liauw, M. A.; Greiner, L. *Org. Process Res. Dev.* **2007**, *11*, 94−97.
(7) (a) Müller, J. J.; Neumann, M.; Scholl, P.; Hilterhaus, L.; Eckstein, M.; Thum, O.; Liese, A. *Anal. Chem.* **2010**, *82*, 6008−6014. (b) Mueller, J. J.; Baum, S.; Hilterhaus, L.; Eckstein, M.; Thum, O.; Liese, A. *Anal. Chem.* **2011**, *83*, 9321−9327.
(8) Franceschini, G.; Macchietto, S. *Chem. Eng. Sci.* **2008**, *63*, 4846−4872.
(9) Heaton, B. *Mechanism in Homogeneous Catalysis, A Spectroscopic Approach*; Wiley-VCH: Weinheim, Germany, 2005; Chapter 4.
(10) Ross, J. *Acc. Chem. Res.* **2003**, *36*, 839−847.
(11) McCann, N.; Phan, D.; Wang, X.; Conway, W.; Burns, R.; Attalla, M.; Puxty, G.; Maeder, M. *J. Phys. Chem. A* **2009**, *113*, 5022−5029.
(12) Wang, X.; Conway, W.; Burns, R.; McCann, N.; Maeder, M. *J. Phys. Chem. A* **2010**, *114*, 1734−1740.
(13) Puxty, G.; Maeder, M.; Rhinehart, R. R.; Alam, S.; Moore, S.; Gemperline, P. *J. Chemom.* **2005**, *19*, 329−340.
(14) Puxty, G.; Neuhold, Y.-M.; Jecklin, M.; Ehly, M.; Gemperline, P. J.; Nordon, A.; Littlejohn, D.; Basford, J. K.; De Cecco, M.; Hungerbühler, K. *Chem. Eng. Sci.* **2008**, *63*, 4800−4809.
(15) Gemperline, P. J.; Puxty, G.; Maeder, M.; Walker, D.; Tarczynski, F.; Bosserman, M. *Anal. Chem.* **2004**, *76*, 2575−2582.
(16) Noda, I. *Vib. Spectrosc.* **2004**, *36*, 143−165.
(17) Noda, I. *J. Mol. Struct.* **2006**, *799*, 2−15.
(18) Noda, I. *J. Mol. Struct.* **2008**, *883*−*884*, 2−26.
(19) Noda, I. *J. Mol. Struct.* **2010**, *974*, 3−24.
(20) (a) Noda, I. *Bull. Am. Phys. Soc.* **1986**, *31*, 520−528. (b) Noda, I. *J. Am. Chem. Soc.* **1989**, *111*, 8116−8118.
(21) Noda, I. *Appl. Spectrosc.* **1993**, *47*, 1329−1336.
(22) Noda, I. *Appl. Spectrosc.* **2000**, *54*, 994−999.
(23) Noda, I.; Ozaki, Y. *Two-Dimensional Correlation Spectroscopy*−*Applications in Vibrational and Optical Spectroscopy*; Wiley: Chichester, West Sussex, England, 2004.
(24) Eads, C. D.; Noda, I. *J. Am. Chem. Soc.* **2002**, *124*, 1111−1118.
(25) Elmore, D. L.; Dluhy, R. A. *J. Phys. Chem. B* **2001**, *105*, 11377−11386.
(26) Shanmukh, S.; Dluhy, R. A. *J. Phys. Chem. A* **2004**, *108*, 5625−5634.
(27) Noda, I. *J. Mol. Struct.* **2006**, *799*, 34−40.
(28) Noda, I.; Allen, W. M.; Lindberg, S. E. *Appl. Spectrosc.* **2009**, *63*, 224−232.
(29) (a) Šašić, S.; Muszynski, A.; Ozaki, Y. *J. Phys. Chem. A* **2000**, *104*, 6380−6387. (b) Segtnan, V. H.; Šašić, S.; Isaksson, T.; Ozaki, Y. *Anal. Chem.* **2001**, *73*, 3153−3161. (c) Šašić, S.; Amari, T.; Ozaki, Y. *Anal. Chem.* **2001**, *73*, 5184−5190.
(30) Taavitsainen, V.-M.; Haario, H. *J. Chemom.* **2001**, *15*, 215−239.
(31) Taavitsainen, V.-M.; Haario, H.; Laine, M. *J. Chemom.* **2003**, *17*, 140−150.
(32) Cornel, J.; Massotti, M. *Anal. Chem.* **2008**, *80*, 9240−9249.
(33) Cornel, J.; Massotti, M. *Ind. Eng. Chem. Res.* **2009**, *48*, 10740−10745.
(34) Dittmar, K.; Siesler, W. H. *Fresenius' J. Anal. Chem.* **1998**, *362*, 109−113.
(35) Friebe, A.; Siesler, H. W. *Vib. Spectrosc.* **2007**, *43*, 217−220.
(36) Spegazzini, N.; Siesler, H. W.; Ozaki, Y. *J. Phys. Chem. A* **2011**, *115*, 8832−8844.
(37) Noda, I. *J. Mol. Struct.* **2010**, *974*, 108−115.
(38) Savitzky, A.; Golay, M. J. E. *Anal. Chem.* **1964**, *36*, 1627−1639.
(39) Furusjö, E.; Danielsson, L.-G. *Chemom. Intell. Lab. Syst.* **2000**, *50*, 63−73.
(40) (a) Connors, K. A. *Chemical Kinetics: The Study of Reaction Rates in Solution*; VCH Publishers: New York, 1990; Chapter 5. (b) Atkins, P.; De Paula, J. *Physical Chemistry*, 9th ed.; Oxford University Press: Oxford, U.K., 2010; Chapter 22.